

Application of stable isotope analysis for improved understanding of the methane budget: comparison of TROICA measurements with TM3 model simulations

Oksana A. Tarasova · Sander Houweling · Nikolai Elansky · Carl A. M. Brenninkmeijer

Received: 8 February 2010 / Accepted: 15 April 2010 /
Published online: 5 May 2010
© Springer Science+Business Media B.V. 2010

Abstract Presented is a detailed comparison of CH₄ and δ¹³C–CH₄ measurements with simulations of the global transport model TM3. Experimental data were obtained during campaigns along the Trans-Siberian railroad in the framework of the TROICA project. Two summer (1999 and 2001) and one spring (2003) expeditions are evaluated. Model simulations include sensitivity tests to further investigate the isotopic composition of natural gas and emissions from Siberian wetlands. Comparison of the average mixing ratio of methane and its isotopic composition (δ¹³C) has been performed for different geographic zones, including the European part of Russia, Western Siberia and Central Siberia. Simulations are in reasonable agreement with the measurements for the European part of Russia and confirm a high contribution of natural gas to the observed methane levels. An increase of emission from bogs shifts the simulated methane isotopic composition closer to the observations. The relative importance of the Western Siberia emissions in current inventories is underestimated in comparison with other wetland regions in the former USSR. Simulated average mixing ratios are in a good agreement with the observations in Central Siberia, while ¹³C(CH₄) values tend to be higher than measured in all considered scenarios. These results point to a bias in the modeled source mixture over Russia, which could be repaired by shifting emissions from isotopically heavy methane sources (e.g. coal,

O. A. Tarasova (✉)
Atmospheric Environment Research Division, WMO, Geneva, Switzerland
e-mail: otarasova@wmo.int

S. Houweling
SRON Netherlands Institute for Space Research, Utrecht, the Netherlands

S. Houweling
Institute for Marine and Atmospheric Research Utrecht, Utrecht, the Netherlands

N. Elansky
Obukhov Institute of Atmosphere Physics RAS, Moscow, Russia

C. A. M. Brenninkmeijer
Max Planck Institute for Chemistry, Mainz, Germany

oil or biomass burning) to light sources (e.g. wetlands, ruminants, waste treatment). Alternatively, the average isotopic signature of Siberian wetlands may be lighter than expected.

Keywords Atmospheric methane · Isotopic analysis · Measurements · Modeling · Russia

1 Introduction

Methane is the third most important greenhouse gas in the Earth's atmosphere after carbon dioxide and water vapor. It contributes 18.2% to the increase in overall global radiative forcing since 1750 caused by all long-lived greenhouse gases (WMO/GAW, GHG Bulletin, 2009). During the late 1980s, the global methane mixing ratio increased at a rate of up to 13 ppb per year and a new steady state mixing ratio was reached around the year 2000, as reported by Dlugokencky et al. (2003). Since then global methane has shown substantial inter-annual variability, without a significant trend. In 2008 the global average mixing ratio was the highest since the stabilization phase (WMO/GAW GHG Bulletin 2009), which can either be the start of a new "methane growth phase" (Rigby et al. 2008) or another example of the inter-annual variability. The growth rate variability of atmospheric methane is connected with variability in natural emissions (for example, variations in wetlands emissions), sinks (variations in OH) and atmospheric transport.

Several studies have investigated the global budget of methane by combining the measurements from the global monitoring networks with results from chemistry transport models applying both forward and inverse approaches (Fiore et al. 2006; Houweling et al. 1999, 2006; Chen and Prinn 2006; Bousquet et al. 2006; Bergamaschi et al. 2005). Nevertheless the observed methane mixing ratio changes remain poorly understood in large part because of paucity of in situ measurements (Nisbet 2007).

The substantial uncertainties in modeling are associated with assumptions regarding methane sources while uncertainties associated with atmospheric transport depend on scale. The large scale patterns are fairly well resolved by models (although even there transport errors may cause biases). On the regional scale the influence of transport uncertainties may be substantial (i.e. not necessarily much less important than that of the unresolved emissions).

Microbial methane production (in natural environments or associated with human activities, such as agriculture) accounts for 70% of the global methane emissions. Natural wetlands are the largest and the most uncertain source category, which are estimated to emit between 115 and 260 TgCH₄ yr⁻¹ (Wang et al. 2004). In the scenario considered in the paper total wetland emissions (swamps and bogs) constitute 184.2 TgCH₄ yr⁻¹. Western Siberia accounts for about 20% of the global wetland emissions (Aselmann and Crutzen 1989; Kuhlmann et al. 1998; Worthy et al. 1999; Bohn et al. 2007).

Russia contributes significantly to the global methane budget not only because it hosts an extensive wetland area, but also because it is the largest natural gas producing country in the world. According to the estimates of Reshetnikov et al. (2000) natural gas production and consumption in Russia release 26.1 to 36.7 TgCH₄ yr⁻¹ (37 to 52 billion m³ of methane under STP) in the atmosphere. More recent comprehensive studies demonstrated much lower (about 10 times) methane leakages (Lechtenboehmer et al. 2005; Lelieveld et al. 2005). They point out that leakages and service releases of natural gas from the high-pressure pipelines of Gazprom constitute about 0.7% (within the range of 0.4 to 1.6%) of the gas transported over long-distance and are mostly from compressor stations. The

aforementioned studies, which were limited to the high-pressure gas transport from West Siberia to Europe (by Gazprom) did not account for low-pressure distribution nets and natural gas emissions from oil and coal exploitation. Gas distribution networks in cities are likely to be leaking, which is confirmed by the regular high peaks in methane concentration registered at the parts of the railroad crossing urban areas.

In addition to the substantial uncertainty of the estimates of the primary methane sources, some smaller sources have to be accommodated within the regional budgets. For example, the work of Walter et al. (2006) shows the particular relevance for Russian ecosystems the ebullition from decomposing thaw lake sediments in north Siberia (with estimated flux of $3.8 \text{ Tg CH}_4 \text{ yr}^{-1}$).

Measurements of stable isotope ratios of carbon ($^{13}\text{C}/^{12}\text{C}$) and hydrogen (D/H) in atmospheric CH_4 can help to reduce the uncertainties of CH_4 emission estimates by constraining the relative importance of isotopically distinct source categories (Fischer et al. 2008). There is a clear differentiation of $\delta^{13}\text{C}$ – δD signatures between three principal methane sources: 1) biogenic (bacterial/microbial) methane formation; 2) thermogenic formation, and 3) biomass burning. In general the biogenic processes of CH_4 production are characterised by low $\delta^{13}\text{C}$ and δD values ($\delta^{13}\text{C} \sim -60\text{‰ VPDB}$ and $\delta\text{D} \sim -310\text{‰ VSMOW}$) compared with other sources. Lassey et al. (2007 and references therein) showed that application of stable isotope analysis to atmospheric modelling can substantially improve the estimated source composition.

The aim of our paper is to improve the understanding of the global methane budget by comparing measurements of methane and its ^{13}C isotope along the Trans-Siberian railroad with results from the global transport model TM3 (Heimann and Koerner 2003; Houweling et al. 2006).

2 Data and methodology

2.1 Methane and its stable isotope measurements

Surveys along the Trans-Siberian railway are carried out on a semi-regular basis since 1995 as part of the TROICA project (Trans-Siberian Observations into the Chemistry of the Atmosphere). Here a train is used as a platform for the atmospheric measurements. Details of the measurements, analytical work and results can be found elsewhere (Crutzen et al. 1998; Bergamaschi et al. 1998; Röckmann et al. 1999; Oberlander et al. 2002; Hurst et al. 2004; Tarasova et al. 2005, 2006, 2007; Belikov et al. 2006; Turnbull et al. 2009). General information about the project is available on the web at www.troica-environmental.com and www.troica.ru.

We utilize measurements of methane from a continuous monitoring system on board of the train and of methane stable isotope ratios ($\delta^{13}\text{C}$) analyzed in air samples, which were collected during the journey. Three campaigns are considered for comparison with model simulations, namely TROICA 5 (referred to in the text as T5), TROICA 7 (T7) and TROICA 8 (T8). The routes and dates of the measurements are given in Table 1. For the T5 campaign continuous measurements were performed by gas chromatography with Flame Ionization Detection (GC-FID, Shimadzu-8A). For the T7 and T8 campaigns the continuous methane measurements were performed using a 4-channel Airborne Chromatograph for Atmospheric Trace Species (ACATS-IV) (Hurst et al. 2004). All methane measurements are performed on the same scale (CMDL, used before NOAA04). A detailed description of the air sampling and methane isotopic composition measurements can be

Table 1 Time and routes of the TROICA campaigns which measurements are used in the paper

Experiment	Time	Route
TROICA-5	26 June–2 July, 3–7 July, 11–13 July 1999	N. Novgorod - Khabarovsk Khabarovsk–Novosibirsk Novosibirsk–Moscow
TROICA-7	27 June–3 July, 4–10 July 2001	Moscow–Khabarovsk Khabarovsk–Moscow
TROICA-8	19–25 March, 26 March–1 April 2004	Moscow–Khabarovsk Khabarovsk–Moscow

found in Tarasova et al. (2006, 2007) and references therein. The isotopic composition of methane is given in delta notation ($\delta^{13}\text{C}-\text{CH}_4$) on the VPDB scale. Due to a very limited number of $\delta\text{D}(\text{CH}_4)$ measurements the results of comparison do not provide a substantial contribution to the source analysis and they are not presented in the paper.

2.2 Meteorological information

A back trajectory analysis was conducted to support the interpretation of the TROICA measurements. Back trajectories are calculated using the NIES trajectory model (Maksyutov et al. 2008; Tohjima et al. 2002). The required meteorological data are derived from the NCEP reanalysis at 17 levels and 2.5×2.5 degree resolution at 12 hourly intervals. Arrival points are selected along the railway at 50 km interval. Trajectory arrival level is 600 m above the topography to avoid the impact of the wind shift in the atmospheric boundary layer. Trajectories are calculated to follow fixed pressure levels, but the air parcels are kept at least 300 m above the topography during transport (10 days backward). The trajectory calculation module has been used extensively for analysis of relationship between the atmospheric transport and observed time series of the long-lived tracers such as nitrous oxide (Tohjima et al. 2000), methane (Tohjima et al. 2002) and ozone (Pochanart et al. 2001). Figure 1 presents the trajectories that were calculated for the TROICA campaigns considered in this study.

In addition to the trajectory analysis, the temperature gradient in the lowest 100 m above the train track has been used to determine the stability of the atmospheric boundary layer. The air temperature gradient was estimated based on data obtained from an ATTEX MTP-5 micro-wave profiler installed in the TROICA measurement wagon. The instrument consists of a state-of-the-art 5 mm wavelength receiver and signal processing software. The profiler measures air temperature at 13 levels in the lowermost 600 m with a repeat cycle of 120 s. Temperature gradient data are available for all campaigns discussed in the paper.

2.3 Model description and scenarios

Global methane simulations were performed with the TM3 model (Heimann and Koerner 2003; Houweling et al. 2006) using meteorological fields from the NCEP reanalysis project (Kalnay et al. 1996). Simulations were carried out on a spatial grid of 4° latitude \times 5° longitude and at 19 hybrid sigma-pressure levels. Hourly concentrations were stored for a sub-domain covering the track of the Trans-Siberian railroad, from which TROICA samples were collected by linear interpolation to the times and locations of the measurements. It

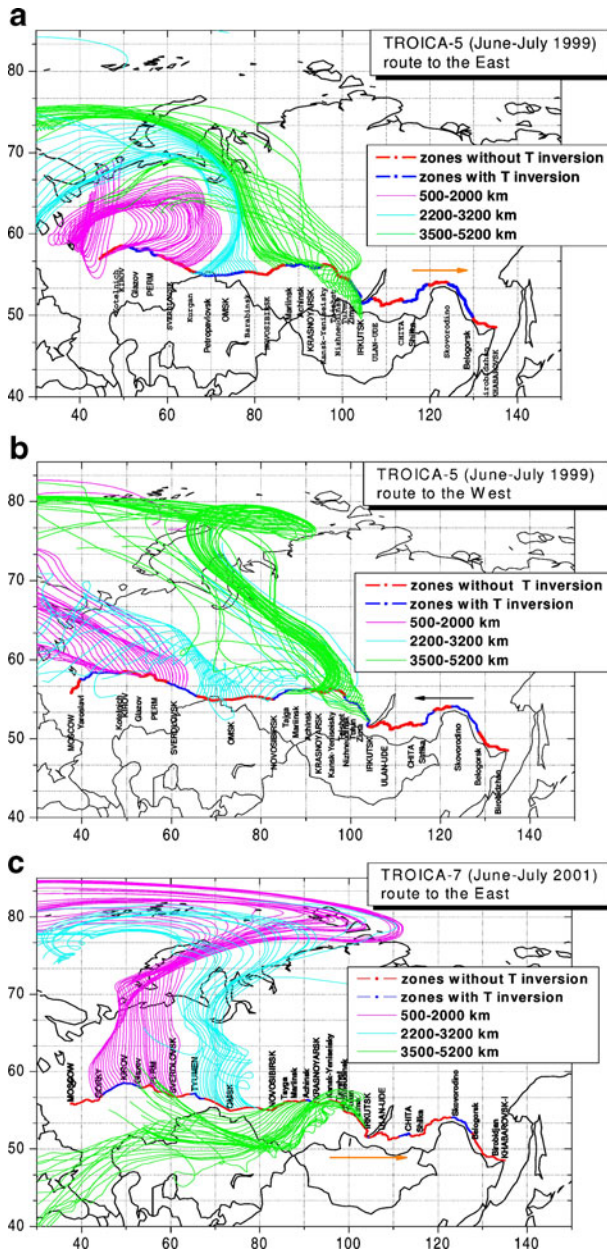


Fig. 1 Air masses back trajectories arriving at the Trans-Siberian rail road at the time of the measurements. Trajectories arriving to different zones as described in the text are plotted in different colors. The rail road is marked by red color if temperature decreases with altitude in the lowest 100 m, while blue colored parts of the railway correspond to the zones with temperature inversion (temperature increase with the altitude in the lowest 100 m). Figures correspond to different campaigns as follows: **a** is T5 to the East, **b** is T5 to the West, **c** is T7 to the East, **d** is T7 to the West, **e** is T8 to the East and **f** is T8 to the West. Cities along the route are indicated below the railroad line

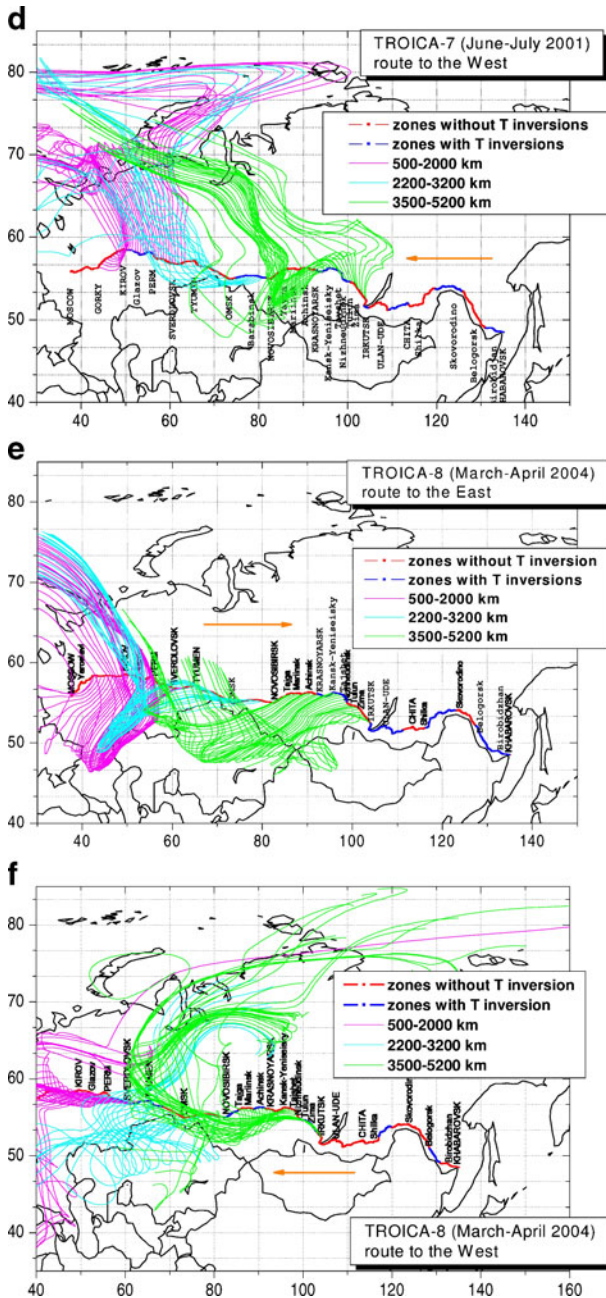


Fig. 1 (continued)

should be noted that sampling procedure includes diurnal variability of the atmospheric methane, caused by variations of the PBL height. Sources and sinks of methane and their isotopic compositions were specified as described in Houweling et al. (2006) with the exception of anthropogenic emissions, which varied during the simulated period according

to the Emissions Database for Global Atmospheric Research (EDGAR) ver.3.2 and EDGAR FT2000 emission inventories (van Aardenne et al. 2000). Figure 2 shows annually mean methane fluxes for two emission categories in the domain, covering Russia. This area covers also big wetland region (emission source) of the Pripayt river system according to Walter et al. (2001) wetland emission inventory which is seen as a high flux area in the middle of the western border of the considered domain. For the base scenario S0 the prescribed emissions together with their isotopic signatures are given in Table 2 for the year 2000. The model calculations included simulation of CH_4 , $\delta^{13}\text{C}(\text{CH}_4)$ and $\delta\text{D}(\text{CH}_4)$, but only CH_4 and $\delta^{13}\text{C}(\text{CH}_4)$ are used for comparison with measurements. A sensitivity calculation (S1) was carried in which the $\delta^{13}\text{C}$ value of natural gas (-40% in the base run S0) was adjusted to that of northern wetlands (-64%). The difference between simulations S0 and S1 highlights the influence of methane emission from natural gas production and distribution. The S1 run is important in particular because the scatter of $\delta^{13}\text{C}(\text{CH}_4)$ for different gas deposits in Western Siberia is large. For example, Dvoretzky et al. (2000)

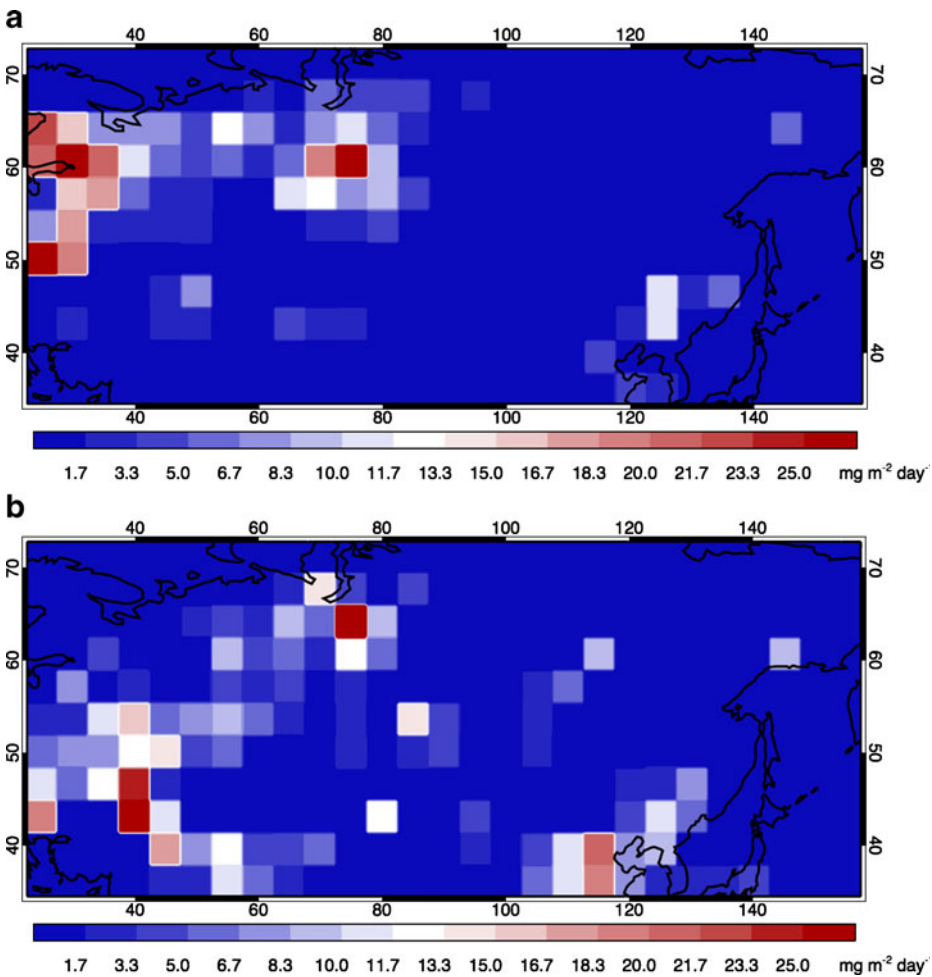


Fig. 2 Annually averaged methane fluxes in the base scenario for two emission categories **a** wetlands and **b** fossil fuel in the year 2000

Table 2 Methane sources and their isotopic composition in the base scenario (S0) of the TM3 global model for the year 2000

Process	Global emission TgCH ₄ /yr	Russian emission TgCH ₄ /yr	δ ¹³ C ‰	δD ‰
Burning	40.2	0.6	-21.8	-200
Rice	38.8	–	-63.0	-335
Soil	-37.8	-2.4		
Termites	19.2	–	-57.0	-300
<i>Bogs^a</i>	37.6	16.3	-64.0	-340
Swamps	149.6	–	-59.0	-315
Coal	33.3	2.2	-35.0	-145
Oil	14.3	1.9	-40.0	-185
Natural gas	43.9	13.4	-40.0	-205
Ruminants	93.4	3.9	-62.0	-310
Waste	59.5	2.5	-55.0	-280
Other ^b	48.0	–		
Sum of all processes	540.0	38.4		

^a For S2 emissions have been increased by 50% in the domain 40N–80N; 30W–140W

^b Includes oceanic and geologic emissions

reported δ¹³C values for methane from the Gasprom exploited deposits (mostly north of 60N and between 70E and 80E) ranging between -64‰ and -34‰, while Cramer et al. (1999) reported δ¹³C values between -55‰ and -34‰ in seeps from Siberian gas fields. Hence, the model sensitivity to the natural gas isotopic composition is expected to be important for the interpretation of comparisons between model simulations and TROICA measurements.

Additional calculations were performed to estimate the sensitivity of the model to biogenic emissions (scenario S2). In this scenario emissions from northern wetlands were increased by 50% within a sub-domain covering the Russian territory north of the Trans-Siberian railroad (40N–80N; 30W–140W).

2.4 Source identification

To identify primary processes contributing to the measured and modeled methane levels a two component mixing model was used. It is based on an assumption that methane observed in the atmosphere consists of contributions from the background and a single (or average) source. The δ¹³C value of this methane source can be determined from a Keeling plot of δ¹³C (CH₄) as a function of the inverse of methane mixing ratio. Commonly, a set of the correlated points is needed to retrieve the intercept of a linear fit to these data, which corresponds to the isotopic composition of the source. If the measurements are performed only at one point (only one measurement/sample is available) or the correlation between δ¹³C and the inverse of methane mixing ratio is poor (e.g. in the case of a heterogeneous mixture of sources with different isotopic ratios) the source isotopic signature can be determined using formula (1) (see for example Köhler et al. 2006) for each individual point:

$$\delta_{CH_4,source} = \frac{C_{obs}\delta_{obs} - C_{bg}\delta_{bg}}{C_{obs} - C_{bg}}, \quad (1)$$

where δ is the $\delta^{13}\text{C}$ or δD isotopic ratio, C is the CH_4 mixing ratio and the subscripts “obs” and “bg” refer to the observed and background values, respectively. As mentioned in Köhler et al. (2006) there are two assumptions underlying this method: 1) the systems consists of only two reservoirs; 2) the isotopic ratio of the carbon in the added reservoir (source) does not change during the time of observations. Both assumptions are only rarely fulfilled, but the derived isotopic signature does characterize the average isotopic signature of the several sources (“mixed source”). The accuracy of the source characterization using formula (1) is influenced by the definition of the background values. Influences of regional sources in the samples that are considered to represent this background can bias the derived isotopic signature of the source.

In the case of simulations the correlation between the inverse of CH_4 mixing ratio and $\delta^{13}\text{C}(\text{CH}_4)$ is used as a criterion for using either a Keeling plot or directly formula (1). If the correlation coefficient exceeds +0.5 the Keeling plot is used, otherwise the source is calculated directly for each individual data point. In case of the latter, the lowest simulated concentration and its isotopic composition is defined as a background. This value varies from case to case. Hence, isotopic signatures of inferred source in the case of the simulated values were derived either from the slope of the Keeling plot or by taking the average value of the estimates obtained with Eq. 1.

In the case of the measurements, the source is estimated for each sample individually with the choice of background mixing ratio and composition as described in Tarasova et al. (2006). These estimates do not depend on the approach, used to estimate the model inferred source.

3 Results and discussion

3.1 General comparison and zone selection

As a first step we compared the continuous measurements of methane mixing ratios with simulated values using scenarios S0 and S2 (S1 differs from the base scenario S0 only by the assumed $\delta^{13}\text{C}$ of natural gas, which does not impact the simulated mixing ratios). For this purpose, the measurement data were smoothed by taking the 100 km median values. The smoothing procedure aimed in removing small-scale variability, which can not be reproduced by the coarse resolution global model. Figure 3 shows examples of the comparison for different campaigns. Note, that interpretation of the performed comparison is rather difficult as datasets contain both the spatial and temporal variability. Hence correlation between measured and simulated mixing ratios is impacted both by difference in the spatial distribution of sources used in the simulations and the real one and in temporal variability of mixing ratios due to unresolved vertical mixing or horizontal advection.

Spatial resolution of the TM3 model used in this exercise restricts its ability to reproduce the local spatial peaks in the observed methane mixing ratio or the amplitude of the variability associated with the diurnal cycle of the PBL height (e.g., methane accumulation under the temperature inversions in the zone of local/regional sources). As a consequence quite low correlation is observed between measured and simulated methane mixing ratios along the whole route (in the range between $R=+0.21$ and $R=+0.60$). The highest correlation is obtained for the spring campaign (T8, eastwards), which has no substantial large-scale (regional) methane peaks. Much lower correlations between measured and simulated methane mixing ratios are found for the summer campaigns (T5 and T7) in comparison with a spring one. In both cases the correlation improves only slightly when increasing the emissions from bogs (S2). The low correlation in summer could be explained

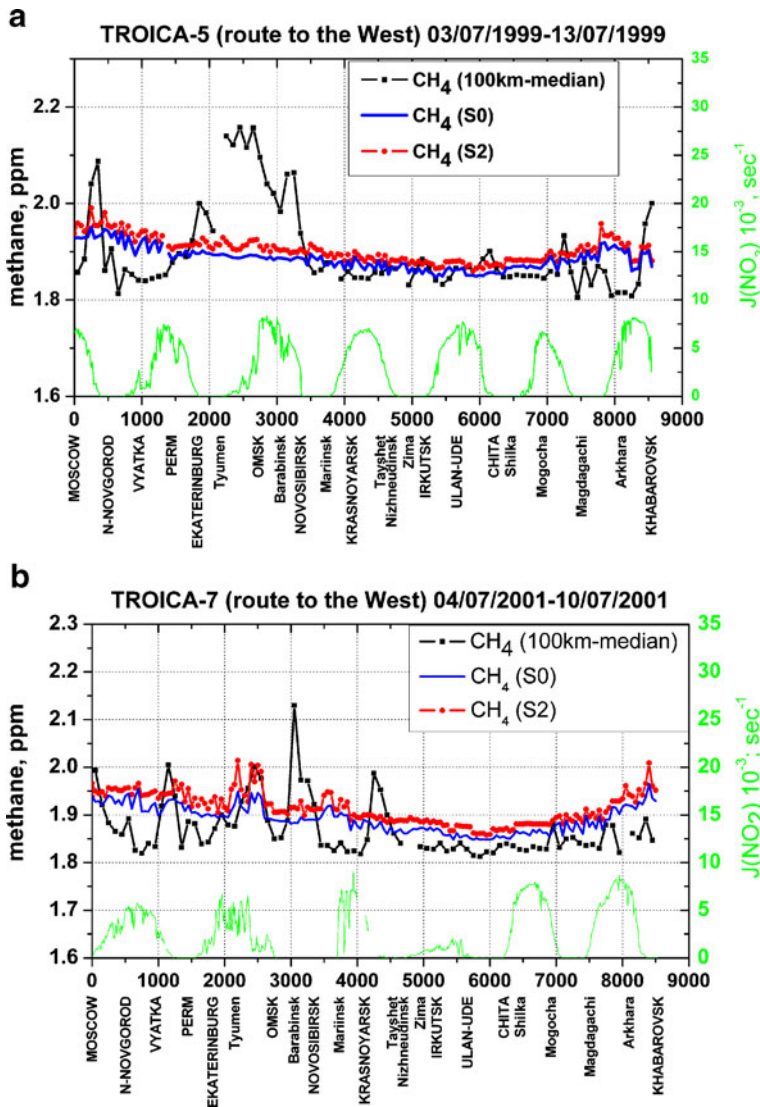


Fig. 3 Comparison of the in situ methane concentration measurements and TM3 simulations in two scenarios (S0 and S2) for **a** route to the West of the TROICA-5 campaign; **b** route to the West of the TROICA-7 campaign and **c** route to the East of the TROICA-8 campaign

by: 1) Underestimated impact of emissions from the West Siberian lowlands (either total fluxes is too low in comparison with the other wetland areas in the considered domain or the emission sources are situated too far to the north relative to the railway to provide a sufficient response); 2) Contributions from unresolved sources/temporal variability along the railway, which could have impacted the measured values but are not captured by the coarse resolution of the model.

The model tends to overestimate the observed methane mixing ratio in the European part of Russia (for summer campaigns) and in the Far East (for all seasons) as shown in Fig. 3. It

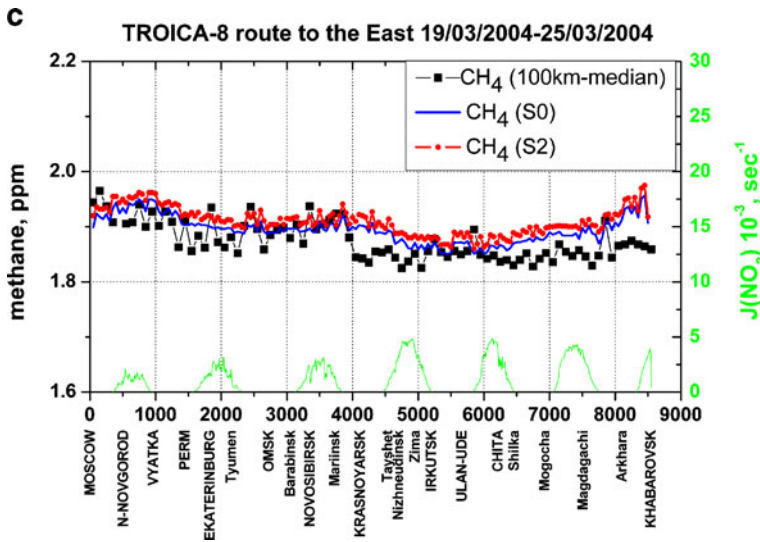


Fig. 3 (continued)

should be noted that due to substantial variability of the measured methane mixing ratios the discussed features are not seen in zone averages, used for analysis in the following chapters. The overestimation over European Russia may be in particular connected with the overestimated or wrongly located emissions in region. In particular the relative importance of the wetland emissions in Ukraine and northern part of the European Russian in the considered base emission scenario seems to be overestimated in comparison with Siberian sources. This non-proportional bogs emission distribution in the country (North-Western corner of the domain where emissions were increased covers the region of St-Petersburg and Karelia) leads to more substantial mixing ratios increase in the scenario of on increased wetland emissions to the West of the country. Moreover, similar overestimate has been reported earlier in comparison of methane concentrations at Pallas, Finland with the simulations by TM5 models using the same wetland emission inventory (Bergamaschi et al. 2005).

Overestimated emissions from China (likely anthropogenic, as this feature is persistent for all seasons) could be considered among the reasons leading to the overestimation of methane mixing ratio at the east of Russia. A similar conclusion was drawn by Meirink et al. (2008) and Bergamaschi et al. (2009) from inverse modeling results using SCIAMACHY data.

A 50% increase of the wetland (bog) emissions in scenario S2 causes an average increase of methane mixing ratio of about 15 ppb along the whole transect. This offset is partly explained by the increase in the global background resulting from an adjustment of the global budget (the increased wetland emissions in S2 were not compensated by a reduction in any another source). Disregarding the offset, there is no obvious improvement in the comparison using this scenario due to variety of sources along the railway. To obtain further information on the importance of specific processes we focus the comparison on selected regions for which the primary methane sources are more or less known.

First we discuss a railroad transect between 500 km and 2,000 km from Moscow (about 42E-63E), which crosses the most densely populated region of Russia. In this zone the influence of the natural gas leakages could be substantial (Tarasova et al. 2006) since several large compressor stations and high-pressure gas transportation pipelines are situated near the railway. The largest

compressor station is placed close to Perm and has 10 incoming/outgoing high-pressure pipelines of 1.42 m in diameter. A large gas condensation and storage field is situated in the Perm-Kungur region. There are also several refineries and power stations in the region. In the following we will refer to this region as “industrial zone”.

To investigate the role of northern wetlands we considered a section between 2,200 and 3,200 km from Moscow (about 66E–80E), which crosses the southern edge of Western Siberia and may be only slightly impacted by leakages from gas pipelines. When air is advected from the north, this part of the route is strongly impacted by emissions from the wetlands, which start approximately 100 km to the north of the railway. Nevertheless a certain contribution from anthropogenic sources cannot be excluded because several major cities are situated along the railroad. Although samples in the vicinity of the largest city (Novosibirsk) have been disregarded, several other populated areas can still contribute to the observed methane variability, for example, due to gas leakage from the low-pressure methane distribution networks in the cities. Hereafter we refer to this zone as “Western Siberia”.

According to the observations, Central Siberia is the less impacted by regional methane emissions in comparison with two regions described above. Some methane variability can be expected due to coal mining to the south of the railroad (The Kuznetsky black coal mining region is situated between 53 and 57N, 86E, and several lignite mines are present in the region between 54 and 56N, 88 and 90E). An impact of these sources can be observed if air is advected from the South–South-West of the railroad, especially in the beginning of the zone from Novosibirsk to Achinsk. Except for coal mining, however, the zone between 3,500 and 5,200 km from Moscow (about 84E–104E) represents “semi-background” conditions over the continental mid-latitudes. In the discussion this region is referred to as “Central Siberia”. For this part of the route the best agreement between measured and simulated methane mixing ratios is observed.

3.2 Results for the European part of Russia

Figure 4(a) shows comparisons of measured and model simulated methane mixing ratios for the zone extending from 500 to 2,000 km from Moscow for three campaigns and two emission scenarios. In the following chapters we will compare zone averaged mixing ratios calculated on the basis of the data (measurements of simulations) with the best available resolution (non-smoothed). Zone averaged mixing ratios in the case of measurements are within the range from 1.870 ppm (T8, westward) to 1.994 ppm (T5, eastward). These values exceed the mid latitude background mixing ratio as measured at Mace Head (53.33° N, 9.90°W). At Mace Head, the mean methane mixing ratios were 1.839 ± 0.029 ppm, 1.833 ± 0.019 ppm, and 1.887 ± 0.048 ppm for the periods of the T5, T7 and T8 campaigns respectively (based on the data of AGAGE network <http://agage.eas.gatech.edu/data.htm>).

To make it clear further in the text measured mixing ratios are indexed “M” ($\text{CH}_{4\text{M}}$) and simulated ones with index “S” ($\text{CH}_{4\text{S}}$).

The difference between zone averaged $\text{CH}_{4\text{M}}$ for the summer campaign of 2001 (T7) and the spring campaign of 2004 (T8) is statistically insignificant. It is unclear whether increased methane sources in summer compensate the seasonally increased methane sink because the variability of the methane mixing ratio is large within considered zone for both campaigns. The slight excess of the zone averaged $\text{CH}_{4\text{M}}$ over background for the route to the East of T8 may indicate a regional methane source (likely anthropogenic) in the region or to the south of the railway (Fig. 1e). The average excess of zone average $\text{CH}_{4\text{M}}$ (T8-East) over Mace Head is about 32 ppb, while at several points inside the zone it may reach up to 120 ppb. For the T8-West transect, the average $\text{CH}_{4\text{M}}$ are comparable to Mace Head within the uncertainty.

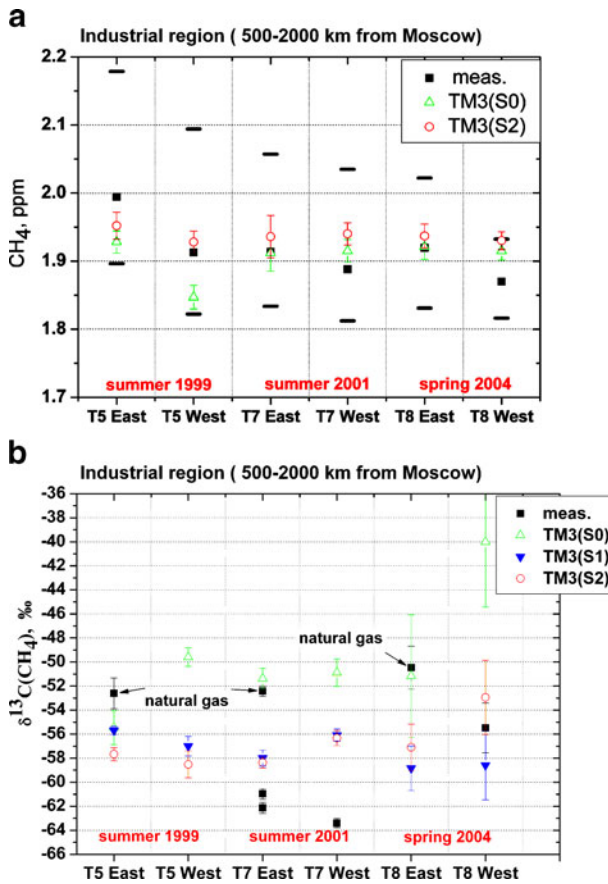


Fig. 4 Comparison of the measured and simulated averaged concentrations and methane inferred sources for the European part of Russia (industrial region, 500–2000 km from Moscow). **a** shows concentrations comparison, while **b** refers to methane source isotopic composition in the campaigns T5, T7 and T8. *Dashes* in **a** show the lowest 5th and the highest 90th percentiles

Small variability of the zone average CH_{4M} for different seasons and for different air transport patterns (compare Fig. 1b–f) indicates the regional origin of the elevated methane levels.

The highest variability of CH_{4M} accompanied by the highest average level is found for the summer campaign of 1999 (T5). The TM3 simulations also provide the highest CH_{4S} for the eastward section of the T5 campaign. This part of the campaign (see Fig. 1a) was characterized by low wind speed in the presence of a persistent anti-cyclone over the European part of Russia. Under these conditions methane is transported from Western Siberian sources to the European part of Russia, where its concentration increases further due to the contribution of local/regional sources. In particular, a temperature inversion formed in the central part of the selected zone (close to Perm with possible gas leakages), could have caused additional methane accumulation in the PBL from sources in vicinity of the railroad. This is confirmed by a substantially elevated methane mixing ratio observed in the central part of the zone.

The largest difference in CH_{4S} between scenarios S0 and S2 for the European part of Russia is found during the T5-West campaign (Fig. 4a). In this case the air was advected

from the North-West (through northern Europe). However, the largest impact of Siberian wetlands is expected for the T5-East, when air is indeed transported from Western Siberia, see Fig. 1(a). This response is not seen in the simulations, but clearly seen in the measurements. Discrepancy points to wetland emissions at the north of the European part of Russia, which are seen in the model response. Hence, we obtained more significant change in CH_4S not coming from Siberian wetland but rather from the sources situated over European Russia. Less sensitivity of CH_4S to the Siberian sources may be due to their underestimated relative contribution in the total wetland emissions in the domain, or more substantial dilution of these emissions in the longer transport from Siberia so that local or closer situated emission sources impact the region to more substantial degree. The latter seems to be less plausible due to long lifetime (about 9 years) of methane in the atmosphere (this effect is not observed in the measurement data).

To further investigate the origin of simulated and observed methane variations, $\delta^{13}\text{C}$ (CH_4) has been analyzed. Inferred source isotopic signatures are presented in Fig. 4(b). The figure shows that in scenario S0 the $\delta^{13}\text{C}(\text{CH}_4\text{S})$ signature of the inferred methane source over European Russia ranges between -55.5 ± 1.4 ‰ and -40.0 ± 5.4 ‰ for different campaigns. The lightest source $\delta^{13}\text{C}(\text{CH}_4\text{S})$ was inferred for the eastward route of the T5 campaign, for which the zone-averaged CH_4S was also the highest. The heaviest, but rather uncertain, $\delta^{13}\text{C}(\text{CH}_4\text{S})$ source is inferred for the spring campaign T8. The large uncertainty in the simulated inferred source points to the presence of multiple sources (presumably anthropogenic) of varying isotopic composition.

Measurements also demonstrate an important contribution of fossil sources to episodes of elevated methane mixing ratios. In fact, the $\delta^{13}\text{C}(\text{CH}_4\text{S})$ value inferred from simulation S0 is very close to $\delta^{13}\text{C}(\text{CH}_4\text{M})$ inferred sources obtained for the observations in the region of strong natural gas leakages (Perm-Kungur). Here we compare the zone average source signature as simulated by model with signatures inferred from individual samples. The $\delta^{13}\text{C}(\text{CH}_4\text{M})$ inferred for the air samples collected in the vicinity of Perm ranges between -52.6 ± 1.3 ‰ and -50.5 ± 1.8 ‰, without a significant difference between spring and summer. Other samples (e.g. from the summer T7 campaign) show much lower $\delta^{13}\text{C}(\text{CH}_4\text{M})$ inferred source signatures, ranging between -64 ‰ and -60 ‰.

To verify the importance of natural gas contribution (in particular coming to the atmosphere through gas leakages) to the simulated methane mixing ratios, the $\delta^{13}\text{C}(\text{CH}_4\text{S})$ of natural gas was adjusted to that of bogs (-65 ‰) and CH_4S and isotopic composition were simulated again (scenario S1). The adjustment caused a proportional to this source contribution change in the isotopic signature of the final atmospheric mixing ratio, namely decrease of the $\delta^{13}\text{C}(\text{CH}_4\text{S})$ inferred source isotopic signature to lower levels than inferred $\delta^{13}\text{C}(\text{CH}_4\text{M})$ in the gas leakage regions, but leaving them higher than inferred $\delta^{13}\text{C}(\text{CH}_4\text{M})$ in the non-leakage regions. This indicates that the adjustment of the isotopic composition of natural gas is supported by the measurements and that, in addition to this, the model either overestimates the relative contribution of methane emissions from isotopically heavy sources or has incorrect isotopic signature of these sources. The impact of adjusting the isotopic value of natural gas is simulated to be the largest for the T8 spring campaign, which is explained by the fact that anthropogenic sources prevail outside the growing season. Substantial response of the $\delta^{13}\text{C}(\text{CH}_4\text{S})$ inferred source signatures on the natural gas isotopic signature adjustment is also found for the summer campaigns (the inferred source gets lighter by up to -7.4 ‰) which confirms that, in the model, natural gas is an important source of methane in this region, also in summer (Fig. 4b).

The increased emissions from bogs in S2 influence the isotopic composition of the $\delta^{13}\text{C}(\text{CH}_4\text{S})$ inferred source differently for the summer and spring campaigns. For the T5 and T7

summer campaigns, the $\delta^{13}\text{C}(\text{CH}_{4\text{S}})$ of the inferred source is depleted by up to 2‰ in comparison with S1. The effect is nearly negligible for T7 and more pronounced for T5. For the summer campaigns, the $\delta^{13}\text{C}(\text{CH}_{4\text{S}})$ of the inferred methane source is more sensitive to the $\delta^{13}\text{C}$ signature of natural gas (comparing S1 and S0) than to increased bogs emissions (comparing S2 and S1). The response on the increased bogs emissions looks different for the spring campaign. The $\delta^{13}\text{C}(\text{CH}_{4\text{S}})$ of the inferred source increases, probably because the emission adjustment influenced the isotopic composition of the background. On the other hand the uncertainty of the $\delta^{13}\text{C}(\text{CH}_{4\text{S}})$ inferred source estimate in the T8 campaign is very big, which does not allow to draw any clear conclusion on the obtained response. As it was mentioned above the spring campaign is very difficult for analysis as methane mixing ratios are controlled by diverse anthropogenic sources on local and regional scale and these sources have different isotopic composition. This leads to extremely poor presentation of the two component mixing model in this case. Inferred methane sources $\delta^{13}\text{C}(\text{CH}_{4\text{M}})$ of the measurements for the spring campaign T8 lay between the results of S1 and S2.

3.3 Results for Western Siberia

A comparison between measured and simulated methane mixing ratios in Western Siberia is shown in Fig. 5(a). As mentioned earlier, this section of the route (2,200–3,200 km) is influenced by wetland emissions (for the position of Siberian wetlands see Peregón et al. 2008). Methane in this zone is advected from the West Siberian lowlands, which starts about 100 km to the north of the railroad. The methane production by wetlands in the region is largely confined to the summer season. Indeed, the continuous measurements in the center of Western Siberia performed by the Institute of Atmosphere Optics in collaboration with NIES in the framework of the TOWER project (Arshinov et al. 2009a) demonstrated a two maxima in the seasonal cycle of methane mixing ratio, namely in spring, caused by the reduced OH sink during winter and in summer, due to wetland emissions. The closer the measurements are to the emission areas the more pronounced is the summer maximum. As soon as the measurement in the TROICA campaign are performed not directly at the area of the wetland but slightly to the south of it, the peak in summer is less pronounced in comparison with central Siberian measurements. The amplitude of the summer seasonal maximum is highly variable due to high sensitivity of methane fluxes from wetlands to meteorological conditions. Aircraft measurements in Western Siberia (Arshinov et al. 2009b) demonstrated higher methane levels in summer 1999 (time of T5) in comparison with the summer 2001 (time of T7), which is also seen in the train measurements.

Figure 5(a) shows that the zone-averaged $\text{CH}_{4\text{M}}$ in Western Siberia are higher for the summer campaigns (T5 and T7) than for the spring campaign (T8). The highest average $\text{CH}_{4\text{M}}$ in this zone are observed during T5, in summer 1999 (about 2.1 ppm for the both routes). A substantial $\text{CH}_{4\text{M}}$ variability is observed for the east route of T5, which is explained by air mass advection from the wetland zone (Fig. 1a) accompanied by methane accumulation under a temperature inversion. Nevertheless, even without a temperature inversion and less efficient transport from northern wetlands (Fig. 1b) a large $\text{CH}_{4\text{M}}$ variability is observed for the west route of T5. The zone average $\text{CH}_{4\text{M}}$ in the T7 campaign only slightly exceeds that of the T8 spring campaign. In spite of the fact that measurements were conducted during different years, the higher mixing ratios in summer compared to spring indicate the presence of a seasonal varying source with a maximum in summer. This source is strong enough to compensate the influence of the seasonally varying large-scale

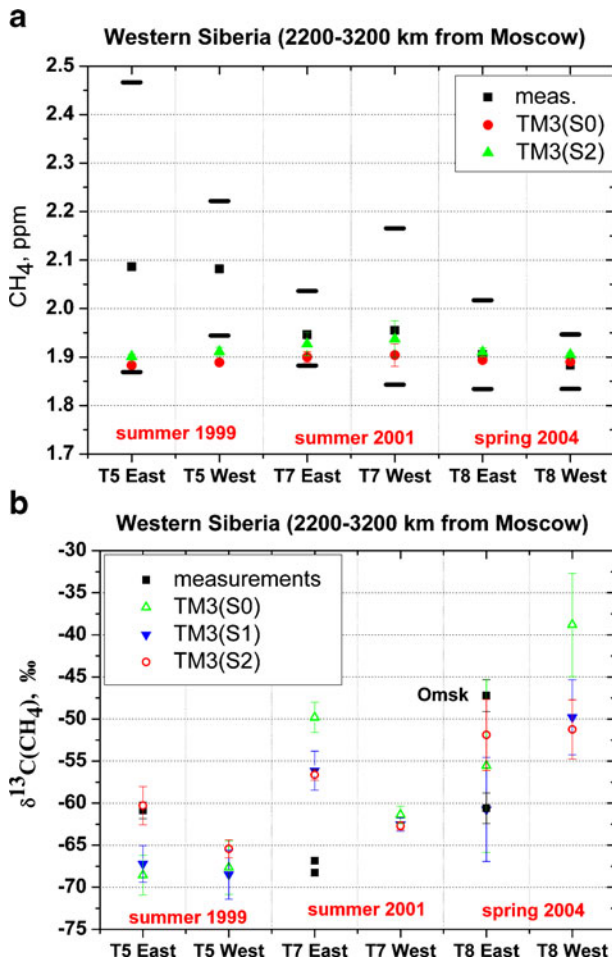


Fig. 5 Comparison of the measured and simulated averaged concentrations and methane inferred sources for Western Siberia (region impacted by wetlands, 2200–3200 km from Moscow). **a** shows concentrations comparison, while **b** refers to methane source isotopic composition in the campaigns T5, T7 and T8. *Dashes* in **a** show the lowest 5th and the highest 90th percentiles

destruction of CH₄ in reaction with OH, which causes a summer minimum in the CH₄ mixing ratio at background sites (Houweling et al. 2000; similar effect was reported for Siberia by Nakazawa et al. 1997). For the spring campaign of 2004 (T8) the zone averaged CH_{4M} are in the range 1.88–1.90 ppm, which is close to the background as measured at Mace Head. Some variability of CH_{4M} is probably due to urban methane sources along the railroad.

It is interesting to note that in spite of the fact that the T5 (1999) and the T7 (2001) campaigns were conducted during the same time of the year, the zone averaged CH_{4M} are substantially different. Taking into consideration the similarity in the air advection patterns for the routes to the east of the T5 and the T7 (Fig. 1a and c) campaigns these results suggest that wetland emissions were higher in 1999 than in 2001 (which is also partly confirmed by Arshinov et al. 2009b). We analyzed several meteorological variables influencing methane emissions from wetlands, namely monthly anomalies of the air

temperature and precipitation (figures are not shown here). Some regional differences were found for the two considered years, in particular a strong positive temperature anomaly over center of Western Siberia in July 1999 and a strong positive precipitation anomaly along the middle stream of Ob river in June 1999. However, it is unclear to what extent these anomalies can explain observed mixing ratio differences, which would require transport model simulations using the output of a process-based wetland model for these specific years.

Comparison of the measured and simulated mixing ratios shows a good agreement for the spring campaign 2004 (T8). Average $\text{CH}_{4\text{S}}$ are underestimated in both emission scenarios (S0 and S2) for the summer campaigns. The most striking discrepancy between zone averaged $\text{CH}_{4\text{S}}$ and $\text{CH}_{4\text{M}}$ is observed for the T5 campaign (summer 1999). Taking into considerations that climatologically average wetland emissions were used for the simulations, the similarity of the simulated mixing ratios in two summers is expected for the same transport patterns, and in fact confirms that observed concentration differences hint to differences in emissions. The most substantial increase of $\text{CH}_{4\text{S}}$ in the S2 scenario, (with increased emissions from bogs), is simulated for the T7 campaign traveling westwards. In this case air is transported from the European part of Russia, Fig. 1d. The response of $\text{CH}_{4\text{S}}$ on the increased emissions is weaker in the case of the direct advection from the wetland region, which occurred in the eastward route of T7. It indicates that the model simulations for this part of the railroad track are not sensitive enough to emissions from Siberian wetlands and wetland emissions are non-proportionally shifted to European wetland/bog sources.

Application of $\delta^{13}\text{C}$ measurements to the Western Siberian dataset provides some additional information on methane sources (Fig. 5b). In the base scenario S0 inferred $\delta^{13}\text{C}$ ($\text{CH}_{4\text{S}}$) source signatures are similarly light as the ones inferred from observation during T5 $\delta^{13}\text{C}(\text{CH}_{4\text{M}})$, but are substantially heavier than the $\delta^{13}\text{C}(\text{CH}_{4\text{M}})$ source inferred for T7 (in particular Eastward route). For the route to the east in summer 2001, the inferred source isotopic signature $\delta^{13}\text{C}(\text{CH}_{4\text{S}})$ for S1 is lighter than that of the base scenario, pointing to a contribution of natural gas to the simulated methane levels. Stronger shift of the inferred $\delta^{13}\text{C}(\text{CH}_{4\text{S}})$ to more depleted values is found for the spring 2004 campaign (T8) due to the prevailing anthropogenic emission during the cold part of the year. The increased methane emissions from wetlands in S2 bring the inferred $\delta^{13}\text{C}(\text{CH}_{4\text{S}})$ source signature in better agreement with the measurements, $\delta^{13}\text{C}(\text{CH}_{4\text{M}})$, in comparison with S1 especially for the east route of the T5 campaign. For the T8 spring campaign, the isotopic signature of local emissions is detected in one of the samples collected in vicinity of Omsk (likely leakages of the low pressure gas distribution networks, giving $\delta^{13}\text{C}_{\text{source}}$ of about -47‰), while under unpolluted conditions the measurements show low values of $\delta^{13}\text{C}_{\text{M}}$ for the inferred source ($-60.6 \pm 1.8\text{‰}$). The fact that the simulations with adjusted isotopic signature of natural gas (S1) and increased emissions from bogs (S2) improve the agreement with the observations basically for summer campaigns allows to conclude that the model underestimates relative role of the light methane sources, overestimates relative role of the heavy methane sources or uses incorrect isotopic composition of methane sources in the basic emission scenario.

3.4 Results for Central Siberia

The section of the route, situated in Central Siberia, is characterized by a weak impact of regional methane sources on the observed methane levels for most wind directions, except for a small part of the route, where South-Western winds advect methane associated with mining in the Kuznetsky coal mining region (see details in chapter 3.1).

Figure 6(a) shows a comparison of the zone averaged $\text{CH}_{4\text{M}}$ and $\text{CH}_{4\text{S}}$ for Central Siberia. Zone averaged $\text{CH}_{4\text{M}}$ are comparable with the background level for the spring campaign (T8) and slightly higher than the background for both summer campaigns (T5 and T7). In general, the agreement between simulated and observed methane mixing ratios is rather good. The highest average methane mixing ratio is found (both in the measurements and in the model) for the eastward transect of the summer 2001 (T7) campaign. The trajectory analysis (Fig. 1c) indicates that air is advected slowly from the south-west crossing a region of intensive coal mining (most of the back trajectories of the samples pass over coal mining activities). The largest variability $\text{CH}_{4\text{M}}$ is observed for the T7 campaign (route to the west), associated with highly non-uniform transport patterns, which leads to contributions from sources in the north of Siberia, from coal mining and accumulation of methane from local sources along the railroad under a temperature inversion. Due to relatively short peaks associated with the mentioned sources the zone averaged $\text{CH}_{4\text{M}}$ for the T7-West is comparable with the zone averaged $\text{CH}_{4\text{M}}$ in the other campaigns.

Analysis of the simulated $\delta^{13}\text{C}(\text{CH}_{4\text{S}})$ source composition of methane (Fig. 6b) shows in general a very low sensitivity to the choice of emission scenario for the summer campaign of 1999 (T5). The inferred sources $\delta^{13}\text{C}(\text{CH}_{4\text{S}})$ are very close to -55‰ for all scenarios (S0, S1, S2). The inferred methane sources $\delta^{13}\text{C}(\text{CH}_{4\text{S}})$ for the T7 summer campaign shows higher sensitivity to the isotopic composition of natural gas (as mentioned above the transport from the north of Western Siberia, where most of Gasprom exploited deposits are situated, may have played a role), while the isotopic composition of the inferred source $\delta^{13}\text{C}(\text{CH}_{4\text{S}})$ gets more depleted after adjustment of the natural gas isotopic signature (S1) and increase of bogs emissions (S2). Measurements nevertheless indicate that biogenic source is the primary inferred source in Central Siberia ($\delta^{13}\text{C}(\text{CH}_{4\text{M}})$ source is in the range between -60‰ and -68‰ for T7). The overestimation of $\delta^{13}\text{C}(\text{CH}_{4\text{S}})$ in the simulations points again to an overestimated contribution from heavy sources (in global budget, as simulations are not sensitive to the regional changes) or an underestimate of light sources or incorrect isotopic composition of the used sources in the basic emission scenario.

Of the spring campaign of 2004 (T8) only one sample from Central Siberia was analyzed for methane isotopic composition. This sample was collected downwind of the coal mining region, as confirmed by its heavy inferred source signature $\delta^{13}\text{C}(\text{CH}_{4\text{M}})$ (Fig. 6b). The inferred sources $\delta^{13}\text{C}(\text{CH}_{4\text{S}})$ from simulation S0 for T8 lays in the range between -33‰ and -53‰ . The upper border of $\delta^{13}\text{C}(\text{CH}_{4\text{S}})$ is even heavier than that of $\delta^{13}\text{C}(\text{CH}_{4\text{M}})$ for coal mining, but it has a large uncertainty. An inferred source isotopic signature $\delta^{13}\text{C}(\text{CH}_{4\text{S}})$ is close to a value of around -45‰ for scenario S2 (after natural gas isotopic signature adjustment and increase of emission from bogs) for both routes of the T8.

4 Summary and conclusions

We investigated the methane budget over Russia utilizing measurements from the TROICA campaigns (Trans-Siberian Observation into the Chemistry of the Atmosphere). Continuous in situ measurements of the methane mixing ratio and measurements of its isotopic composition ($\delta^{13}\text{C}$) were used, as analyzed from air samples collected along the rail road. These measurements are compared with global transport model simulations using the TM3 model. We focus on 3 campaigns: the summer campaigns of 1999 and 2001 (TROICA-5 and -7) and the spring campaign of 2004 (TROICA-8). To support data analysis we used back trajectories to identify the dominant air transport patterns and define qualitatively an impact of different

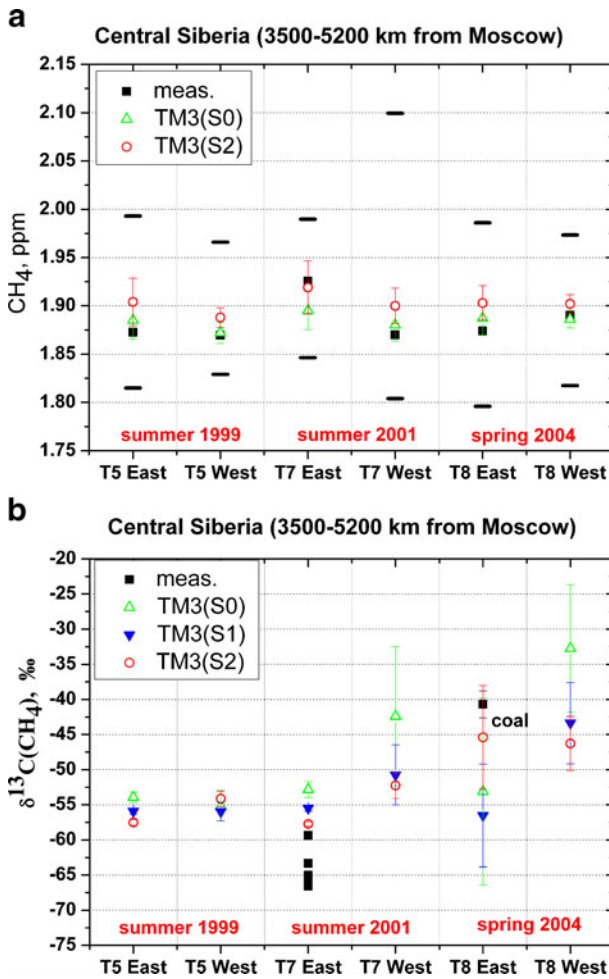


Fig. 6 Comparison of the measured and simulated averaged concentrations and methane inferred sources for Central Siberia (weakly polluted “semi-background” region, 3500–5200 km from Moscow). **a** shows concentrations comparison, while **b** refers to methane source isotopic composition in the campaigns T5, T7 and T8. *Dashes* in **a** show the lowest 5th and the highest 90th percentiles

methane source in selected regions. To further investigate the size and origin of regional sources, different emission scenarios were used and results were analyzed for different geographical zones, namely European part of Russia, Western and Central Siberia. In addition to the standard emission setup (S0) simulations were performed for a scenario with an adjusted isotopic composition of natural gas (in S1 $\delta^{13}\text{C}$ of natural gas was changed from -40‰ to -64‰) and 50% increased emissions from wetlands in the domain north of the Trans-Siberian railroad (40N–80N; 30W–140W). In all runs the anthropogenic emissions include an estimate of the long-term trend, whereas wetland emissions were repeated each year (climatologically averaged). To deduce the inferred source isotopic signature the two components mixing approach was implemented. It should be noted that we used forward simulations in different limited number of scenarios and the conclusions presented here have qualitative (not quantitative) character. Data assimilation techniques are required to use

observations in the model and come up with a-posteriori emission estimates. Considered in the paper measurements dataset does not allow implementation of this approach.

In general, the correlation between the measured and simulated mixing ratios is quite low. This is mainly explained by unresolved emissions and meteorological conditions resulting from the coarse resolution of the global model. We plan to perform further comparison with higher resolution. The best agreement between the measurements and simulations is observed for the spring campaign of 2004 (T8), which is characterized by a rather uniform methane distribution along the expedition route. In general slight overestimate of the observed methane levels by the simulated ones over European Russia is found for summer campaigns and for the Far East for all considered campaigns.

The highest measured and simulated mixing ratios in the European part of Russian are reported for the summer campaign of 1999 (T5). During this campaign the transport conditions (stable anti-cyclone) were favorable for methane transport from Western Siberia. This transport of methane, clearly seen in the measurements, was not reproduced in the simulations. Moreover, the highest model sensitivity to bogs emissions is found in the case of air transport from the north-west of European Russia. This may indicate higher model sensitivity to more regional emissions and overestimated relative role of the wetlands over European part of Russia/Eastern Europe or Finland in comparison with Siberian wetland in the regional methane budget. Analysis of the inferred simulated methane source over European Russia showed a substantial contribution of natural gas to the observed methane levels, which was found to be in a good agreement with measurements. The model showed quite low sensitivity of the simulated methane isotopic composition to increased emissions from bogs for this region.

In Western Siberia the highest methane mixing ratio was observed during the summer campaign of 1999 (T5). For the summer campaign of 2001 (T7) the zone averaged mixing ratio estimated on the basis of measurements is slightly higher than that of the spring campaign of 2004 (T8), indicating the presence of a regional methane source in summer. The simulated mixing ratios are in a good agreement with the measurements for the spring campaign and underestimate the mixing ratios during summer, indicating an underestimated sensitivity to regional wetlands emissions in the model. This may have a concern to a low spatial resolution of the global model. The source signatures inferred from the isotopic measurements clearly indicate methane of biogenic origin in the region. $\delta^{13}\text{C}$ signatures of the sources as inferred from the model span a wide range. The scenario with adjusted natural gas and increased bog emissions (S2) agrees the best with the measurements from the T5 campaign, suggesting that the contribution of the light methane sources is underestimated or that the isotopic signature of wetland emissions is lighter than assumed in the model.

Simulated methane mixing ratios in Central Siberia are in good agreement with the measurements. The isotopic composition of simulated methane is not very sensitive to the choice of emission scenario. Moreover, even with adjusted natural gas isotopic signature (S1) and increased bog emissions (S2) the inferred source signature remains too heavy in comparison with the measurements, consistent with what was found for West Siberia. This could in part be explained by the heavier signature of background methane in the model compared to observations. On average, the increase of the bog emissions improves the agreement between simulated and measured methane isotopic composition, indicate that the simulated source composition should be shifted towards lighter sources.

Acknowledgements We are grateful to the staff of the Institute of Atmospheric Physics, Russia and Dr. Igor B. Belikov in particular for their technical support and carrying out these successful expeditions; Dr. Thomas Röckmann and Dr. Mark Brass (Institute for Marine and Atmospheric Research Utrecht, Utrecht University,

The Netherlands) for performed isotopic measurements, Dr. Patrick Jöckel and Dr. Peter Zimmermann, Max-Planck Institute for Chemistry, Germany, for providing graphical support and creating the TROICA homepage (www.troica-environmental.com); Dr. Dale F. Hurst and Dr. Pavel A. Romashkin, Cooperative Institute for Research in Environmental Sciences, USA, for discussions and in situ methane measurements.

References

- Arshinov, M.Yu., Belan, B.D., Davydov, D.K., Inoue, G., Krasnov, O.A., Maksyutov, S., Machida, T., Fofonov, A.V., Shimoyama, K.: Spatio-temporal variability of CO₂ and CH₄ concentration in the surface atmospheric layer over West Siberia. *Atmos Oceanic Opt* **22**(2), 183–192 (2009a)
- Arshinov, M.Yu., Belan, B.D., Davydov, D.K., Inoue, G., Maksyutov, S., Machida, T., Fofonov, A.V.: Vertical distribution of greenhouse gases over West Siberia from long-term measurement data. *Atmos Oceanic Opt* **22**(5), 457–464 (2009b)
- Aselmann, I., Crutzen, P.J.: Global distribution of natural freshwater wetlands and rice paddies, their net primary productivity, seasonality and possible methane emissions. *J Atmos Chem* **8**, 307–358 (1989)
- Belikov, I., Brenninkmeijer, C.A.M., Elansky, N., Ral'ko, A.: Methane, carbon monoxide, and carbon dioxide concentrations measured in the atmospheric surface layer over continental Russia in the TROICA experiments. *Izvestiya Atmos Ocean Phys* **42**, 46–59 (2006)
- Bergamaschi, P., Brenninkmeijer, C.A.M., Hahn, M., Röckmann, T., Scharffé, D.H., Crutzen, P.J., Elansky, N.F., Belikov, I.B., Trivett, N.B.A., Worthly, D.E.J.: Isotope analysis based source identification for atmospheric CH₄ and CO sampled across Russia using the Trans-Siberian railroad. *J. Geophys. Res.* **103** (D7), 8227–8235 (1998)
- Bergamaschi, P., Krol, M., Dentener, F., Vermeulen, A., Meinhardt, F., Graul, R., Ramonet, M., Peters, W., Dlugokencky, E.J.: Inverse modelling of national and European CH₄ emissions using the atmospheric zoom model TM5. *Atmos Chem Phys* **5**, 2431–2460 (2005)
- Bergamaschi, P., Frankenberg, C., Meirink, J.F., Krol, M., Villani, G.M., Houweling, S., Dentener, F., Dlugokencky, E.J., Miller, J.B., Gatti, L.V., Engel, A., Levin, I.: Inverse modeling of global and regional CH₄ emissions using SCIAMACHY satellite retrievals. Inverse modeling of global and regional CH₄ emissions using SCIAMACHY satellite retrievals. *J. Geophys. Res.* (2009). doi:10.1029/2009JD012287
- Bohn, T.J., Lettenmaier, D.P., Sathulur, K., Bowling, L.C., Podest, E., McDonald, K.C., Friborg, T.: Methane emissions from western Siberian wetlands: heterogeneity and sensitivity to climate change. *Environ Res Letters* **2**(4), 045015 (2007)
- Bousquet, P., Ciais, P., Miller, J.B., Dlugokencky, E.J., Hauglustaine, D.A., Prigent, C., et al.: Contribution of anthropogenic and natural sources to atmospheric methane variability. *Nature* (2006). doi:10.1038/nature05132
- Chen, Y.H., Prinn, R.G.: Estimation of atmospheric methane emissions between 1996 and 2001 using a three-dimensional global chemical transport model. *J. Geophys. Res.* (2006). doi:10.1029/2005JD006058
- Cramer, B., Poelchau, H.S., Gerling, P., Lopatin, N.V., Littke, R.: Methane released from ground-water: the source of natural gas accumulations in northern West Siberia. *Mar. Petrol. Geol.* **16**, 225–244 (1999)
- Crutzen, P.J., Elansky, N.F., Hahn, M., Golitsyn, G.S., Brenninkmeijer, C.A.M., Scharffé, D., Belikov, I.B., Maiss, M., Bergamaschi, P., Röckmann, T., Grisenko, A.M., Sevostyanov, V.M.: Trace gas measurements between Moscow and Vladivostok using the Trans-Siberian Railroad. *J Atmos Chem* **29**(2), 179–194 (1998)
- Dlugokencky, E.J., Houweling, S., Bruhwiler, L., Masarie, K.A., Lang, P.M., Miller, J.B., Tans, P.P.: Atmospheric methane levels off: Temporary pause or a new steady-state? *Geophys. Res. Lett.* (2003). doi:10.1029/2003GL018126
- Dvoretzky, P.I., Goncharov, V.S., Esikov, A.D., Teplinsky, G.I., Il'chenko, V.P.: Isotopic composition of the natural gas at the North of Western Siberia. Information-advertising Centre of Open Stock Company "Gazprom", Series "Geology and Prospecting of gas and gas condensate gas deposits", Moscow, Russia (2000)
- Fiore, A.M., Horowitz, L.W., Dlugokencky, E.J., West, J.J.: Impact of meteorology and emissions on methane trends, 1990–2004. *Geophys. Res. Lett.* (2006). doi:10.1029/2006GL026199
- Fischer, H., Behrens, M., Bock, M., Richter, U., Schmitt, J., Loulergue, L., Chappellaz, J., Spahni, R., Blunier, T., Leuenberger, M., Stocker, T.F.: Changing boreal methane sources and constant biomass burning during the last termination, *Nature* (2008) 452, 864–867, doi:10.1038/nature06825
- Heimann, M., Körner, S.: The global atmospheric tracer model TM3, Model description and user's manual, Release 3.8a, Max Planck Institute of Biogeochemistry, Germany (2003)
- Houweling, S., Kaminski, T., Dentener, F., Lelieveld, J., Heimann, M.: Inverse modeling of methane sources and sinks using the adjoint of a global transport model. *J. Geophys. Res.* **104**(D21), 26137–26160 (1999)

- Houweling, S., Dentener, F.J., Lelieveld, J., Walter, B., Dlugokencky, E.J.: The modeling of tropospheric methane: How well can point measurements be reproduced by a global model? *J. Geophys. Res.* **105** (D7), 8981–9002 (2000)
- Houweling, S., Röckmann, T., Aben, I., Keppler, F., Krol, M., Meirink, J.F., Dlugokencky, E.J., Frankenberg, C.: Atmospheric constraints on global emissions of methane from plants. *Geoph. Res. Letters* (2006). doi:10.1029/2006GL026162
- Hurst, D.F., Romashkin, P.A., Elkins, J.W., Oberländer, E.A., Elansky, N.F., Belikov, I.B., Granberg, I.G., Golitsyn, G.S., Grisenko, A.M., Brenninkmeijer, C.A.M., Crutzen, P.J.: Emissions of ozone-depleting substances in Russia during 2001. *J. Geophys. Res.* (2004). doi:10.1029/2004JD004633
- Kalnay, E., Kanamitsu, M., Kistler, R., Collins, W., Deaven, D., Gandin, L., Iredell, M., Saha, S., White, G., Woollen, J., Zhu, Y., Chelliah, M., Ebisuzaki, W., Higgins, W., Janowiak, J., Mo, K.C., Ropelewski, C., Wang, J., Leetmaa, A., Reynolds, R., Jenne, R., Joseph, D.: The NCEP/NCAR 40-year reanalysis project. *Bull. Am. Met. Soc.* **77**, 437–471 (1996)
- Köhler, P., Fischer, H., Schmitt, J., Munhoven, G.: On the application and interpretation of Keeling plots in paleo climate research—deciphering $\delta^{13}\text{C}$ of atmospheric CO_2 measured in ice cores. *Biogeosciences* **3**, 539–556 (2006)
- Kuhlmann, A.J., Worthy, D.E.J., Trivett, N.B.A., Levin, I.: Methane emissions from a wetland region within the Hudson Bay lowland: an atmospheric approach. *J. Geophys. Res.* **103**(D13), 16 (1998). 009-16.016
- Lassey, K.R., Etheridge, D.M., Lowe, D.C., Smith, A.M., Ferretti, D.F.: Centennial evolution of the atmospheric methane budget: what do the carbon isotopes tell us? *Atmos. Chem. Phys.* **7**, 2119–2139 (2007)
- Lechtenboehmer, S., Dienst, C., Fishedick, M., Hanke, T., Akopova, G., Gladkaja, N., Assonov, S.: GHG-emissions of Russian natural gas industry by gas export to Europe. Presented at NCGG-4, Utrecht (2005)
- Lelieveld, J., Lechtenböhmer, S., Assonov, S.S., Brenninkmeijer, C.A.M., Dienst, C., Fishedick, M., Hanke, T.: Greenhouse gases: Low methane leakage from gas pipelines. *Nature* **434**, 841–842 (2005)
- Maksyutov, S., Patra, P.K., Onishi, R., Saeki, T., Nakazawa, T.: NIES/FRCGC Global Atmospheric Tracer Transport Model: Description, Validation, and Surface Sources and Sinks Inversion. *J Earth Simulator* **9**, 3–18 (2008)
- Meirink, J.F., Bergamaschi, P., Frankenberg, C., d’Amelio, M.T.S., Dlugokencky, E.J., Gatti, L.V., Houweling, S., Miller, J.B., Röckmann, T., Villani, G.M., Krol, M.C.: Four-dimensional variational data assimilation for inverse modeling of atmospheric methane emissions: Analysis of SCIAMACHY observations. *J. Geophys. Res.* (2008). doi:10.1029/2007JD009740
- Nakazawa, T., Sugawara, S., Inoue, G., Machida, T., Makshyutov, S., Mukai, H.: Aircraft measurements of the concentrations of CO_2 , CH_4 , N_2O , and CO and the carbon and oxygen isotopic ratios of CO_2 in the troposphere over Russia. *J. Geophys. Res.* **102**(D3), 3843–3859 (1997)
- Nisbet, E.: Earth monitoring: Cinderella science. *Nature* (2007). doi:10.1038/450789a
- Oberlander, E.A., Brenninkmeijer, C.A.M., Crutzen, P.J., Elansky, N.F., Golitsyn, G.S., Granberg, I.G., Scharffe, D.H., Hofman, R., Belikov, I.B., Paretzke, H.G., van Velthoven, P.: Trace gas measurements along the Trans-Siberian railroad, the Troica 5 expedition. *J. Geophys. Res.* (2002). doi:10.1029/2001JD000953
- Peregon, A., Maksyutov, S., Kosykh, N.P., Mironycheva-Tokareva, N.P.: Map-based inventory of wetland biomass and net primary production in western Siberia. *J. Geophys. Res.* (2008). doi:10.1029/2007JG000441
- Pochanart, P., Akimoto, H., Maksyutov, S., Staehelin, J.: Surface ozone at the Swiss alpine site Arosa: the hemispheric background and the influence of the large scale atmospheric emissions. *Atmos. Environ.* **35**, 5553–5566 (2001)
- Reshetnikov, A.I., Paramonova, N.N., Shashkov, A.A.: An evaluation of historical methane emissions from the Soviet gas industry. *J. Geophys. Res.* **105**(3), 517–529 (2000)
- Rigby, M., Prinn, R.G., Fraser, P.J., Simmonds, P.G., Langenfelds, R.L., Huang, J., Cunnold, D.M., Steele, L. P., Krummel, P.B., Weiss, R.F., O’Doherty, S., Salameh, P.K., Wang, H.J., Harth, C.M., Mühle, J., Porter, L.W.: Renewed growth of atmospheric methane. *Geophys. Res. Lett.* (2008). doi:10.1029/2008GL036037
- Röckmann, T., Brenninkmeijer, C.A.M., Hahn, M., Elansky, N.F.: CO mixing and isotope ratios across Russia; Trans-Siberian Railroad Expedition TROICA 3, April 1997. *Chemosphere* **1**, 219–231 (1999)
- Tarasova, O.A., Brenninkmeijer, C.A.M., Assonov, S.S., Elansky, N.F., Hurst, D.F.: Methane variability measured across Russia during TROICA expeditions. *Environ. Sci.* **2**(2–3), 241–251 (2005)
- Tarasova, O.A., Brenninkmeijer, C.A.M., Assonov, S.S., Elansky, N.F., Röckmann, T., Brass, M.: Atmospheric CH_4 along the Trans-Siberian Railroad (TROICA) and River Ob: Source Identification using Stable Isotope Analysis. *Atmos. Environ.* **40**(29), 5617–5628 (2006)
- Tarasova, O.A., Brenninkmeijer, C.A.M., Assonov, S.S., Elansky, N.F., Röckmann, T., Sofiev, M.A.: Atmospheric CO along the Trans-Siberian railroad and river Ob: Source identification using isotope analysis. *J. Atmos. Chem.* **57**(2), 135–152 (2007)

- Tohjima, Y., Mukai, H., Maksyutov, S., Takahashi, Y., Machida, T., Utiyama, M., Katsumoto, M., Fujinuma, Y.: Variations in atmospheric nitrous oxide observed at Hateruma monitoring station. *Chemosphere—Global Change. Science* **2**, 435–443 (2000)
- Tohjima, Y., Machida, T., Utiyama, M., Katsumoto, M., Fujinuma, Y., Maksyutov, S.: Analysis and presentation of in situ atmospheric methane measurements from Cape Ochishi and Hateruma Island. *J. Geophys. Res.* **107**(D12), 4148 (2002)
- Turnbull, J.C., Miller, J.B., Lehman, S.J., Hurst, D., Peters, W., Tans, P.P., Southon, J., Montzka, S.A., Elkins, J.W., Mondeel, D.J., Romashkin, P.A., Elansky, N., Skorokhod, A.: Spatial distribution of $\Delta^{14}\text{C}\text{O}_2$ across Eurasia: measurements from the TROICA-8 expedition. *Atmos. Chem. Phys.* **9**, 175–187 (2009)
- van Aardenne, J.A., Dentener, F.J., Olivier, J.G.J., Peters, J.A.H.W., Ganzeveld, L.N.: The EDGAR 3.2 Fast track 2000 dataset (32FT2000), Joint Research Centre (JRC), Ispra, Italy, available from <http://www.mnp.nl/edgar/model/v32ft2000edgar> (2005)
- Walter, B.P., Heimann, M., Matthews, E.: Modeling modern methane emissions from natural wetlands I. Model description and results. *J. Geophys. Res.* **106**(D24), 34189–34206 (2001)
- Walter, K.M., Zimov, S.A., Chanton, J.P., Verbyla, D., Chapin, F.S.: Methane bubbling from Siberian thaw lakes as a positive feedback to climate warming. *Nature* **443**(7107), 71–75 (2006)
- Wang, J.S., Logan, J.A., McElroy, M.B., Duncan, B.N., Megretskaja, I.A., Yantosca, R.M.: A 3-D model analysis of the slowdown and interannual variability in the methane growth rate from 1988 to 1997. *Glob. Biogeochem. Cycles* (2004). doi:[10.1029/2003GB002180](https://doi.org/10.1029/2003GB002180)
- WMO Greenhouse Gas Bulletin: The State of Greenhouse Gases in the Atmosphere Using Global Observations through 2008, No.5. WMO, Geneva (2009)
- Worthy, D.E.J., Levin, I., Trivett, N.B.A., Kuhlmann, A.J., Hopper, J.F., Ernst, M.K.: Seven years of continuous methane observations at a remote boreal site in Ontario, Canada. *J. Geophys. Res.* **103**(D13), 15995–16007 (1999)